



Perpendicular-bias-field-dependent vortex-gyration eigenfrequency

Myoung-Woo Yoo, Ki-Suk Lee, Dong-Soo Han, and Sang-Koog Kim

Citation: *Journal of Applied Physics* **109**, 063903 (2011); doi: 10.1063/1.3563561

View online: <http://dx.doi.org/10.1063/1.3563561>

View Table of Contents: <http://scitation.aip.org/content/aip/journal/jap/109/6?ver=pdfcov>

Published by the [AIP Publishing](#)

Articles you may be interested in

[Micromagnetic simulations of magnetic normal modes in elliptical nanomagnets with a vortex state](#)

Appl. Phys. Lett. **103**, 252404 (2013); 10.1063/1.4850537

[Magnetic vortex echoes](#)

J. Appl. Phys. **112**, 113911 (2012); 10.1063/1.4768446

[Radial-spin-wave-mode-assisted vortex-core magnetization reversals](#)

Appl. Phys. Lett. **100**, 172413 (2012); 10.1063/1.4705690

[Sub-nanosecond switching of vortex cores using a resonant perpendicular magnetic field](#)

Appl. Phys. Lett. **100**, 082402 (2012); 10.1063/1.3687909

[Limits for the vortex state spin torque oscillator in magnetic nanopillars: Micromagnetic simulations for a thin free layer](#)

J. Appl. Phys. **108**, 123914 (2010); 10.1063/1.3524222

A horizontal banner with an orange-to-yellow gradient background. The text '2014 Special Topics' is centered in a large, white, sans-serif font. Below the text are five circular icons, each containing a different material structure and a label: 'PEROVSKITES' (red and black geometric shapes), '2D MATERIALS' (blue and red grid), 'MESOPOROUS MATERIALS' (green and blue porous structure), 'BIOMATERIALS/ BIOELECTRONICS' (yellow and black grid), and 'METAL-ORGANIC FRAMEWORK MATERIALS' (brown and black porous structure). At the bottom left is the 'AIP | APL Materials' logo. At the bottom right is a red ribbon with the text 'Submit Today!' in white.

2014 Special Topics

PEROVSKITES

2D MATERIALS

MESOPOROUS MATERIALS

BIOMATERIALS/ BIOELECTRONICS

METAL-ORGANIC FRAMEWORK MATERIALS

AIP | APL Materials

Submit Today!

Perpendicular-bias-field-dependent vortex-gyration eigenfrequency

Myoung-Woo Yoo, Ki-Suk Lee, Dong-Soo Han, and Sang-Koog Kim^{a)}

Research Center for Spin Dynamics & Spin-Wave Devices, Nanospinics Laboratory, Research Institute of Advanced Materials, Department of Materials Science and Engineering, Seoul National University, Seoul 151-744, South Korea

(Received 13 January 2011; accepted 22 January 2011; published online 17 March 2011)

We found that the angular frequency ω_0 of vortex-core gyrations is controllable by the application of static perpendicular bias fields H_p as studied by micromagnetic simulations and Thiele's approach-based quantitative interpretation. The observed linear dependence of ω_0 on H_p could be explained in terms of the dynamic variables of the vortex, the gyrovectored constant G , and the potential stiffness constant κ , for cases of negligible damping. Here we calculated the values of G and κ as a function of H_p directly from the simulation numerical data using Thiele's equivalent force equations, providing a more correct understanding of the remarkable change of ω_0 with H_p . This micromagnetic-simulation-based quantitative analysis is a straightforward, accurate, and effective means of understanding vortex dynamics in nanoscale magnetic elements. © 2011 American Institute of Physics.

[doi:10.1063/1.3563561]

I. INTRODUCTION

Magnetic vortex configurations have received a great deal of attention, not only because of the vortex structure's unique fourfold ground states in magnetic nanodots of micrometer size or smaller^{1,2} but also due to its nontrivial vortex-core reversal dynamics.^{3–7} The fourfold vortex states are represented by combinations of either counter-clockwise (CCW) or clockwise (CW) in-plane curling magnetization and either up- or downward out-of-plane magnetization at the core.¹ Owing not only to the binary representation of the core orientation⁸ but also to the full degrees of freedom of the fourfold ground states,⁹ such a stable vortex structure has been considered as a candidate for potential information storage applications.¹⁰ Furthermore, the existence of the vortex core, combined with the restoring force associated with nanodots' finite lateral size, gives rise to in-plane rotating motions of the core around its equilibrium center position at the characteristic angular eigenfrequency ω_0 in either the CCW or CW angular rotation direction, so-named the gyrotropic mode.¹¹ Such persistent vortex oscillations, with their high power output and narrow line widths, have been studied intensively recently for their promising application to microwave emission sources.¹²

It is well known that the rotation sense of the gyrotropic mode is determined by the core magnetization direction¹¹ and that the value of ω_0 depends on the dot dimensions, that is, thickness-to-radius (L/R) ratio for the given material.¹³ ω_0 typically falls within the 50–600 MHz range for L/R ratios between 0.01 and 0.12.¹³ The ω_0 , then, is not controllable for a given dot. Finding a way to manipulate it with external parameters such as fields, meanwhile, is a challenge. Choi *et al.*¹⁴ reported that the eigenfrequency can be modified by Oersted fields produced by an out-of-plane dc current, specifically by varying the potential energy of the dots. Very

recently, Loubens *et al.*¹⁵ reported an experimental observation of the dependence of ω_0 on the strength of a static magnetic field H_p applied perpendicularly to the nanodot plane. However, the underlying physics have yet to be quantitatively unraveled. In this paper, we report, on the basis of micromagnetic simulations, that the value of ω_0 is controllably variable linearly with H_p in its sufficiently wide but limited range. Furthermore, this work provides a more correct understanding of the linear dependence of ω_0 on H_p as determined by direct calculation of the H_p dependences of the dynamic variables of the vortex through Thiele's equivalent force equation,¹⁶ using the numerical simulation data.

II. MODELING AND MICROMAGNETIC SIMULATION

In the present micromagnetic simulations, we used the OOMMF code¹⁷ implementing the Landau–Lifshitz–Gilbert (LLG) equation¹⁸ of motion. We chose, for the model system, a permalloy (Py: Ni₈₀Fe₂₀) nanodisk of 300 nm radius and 30 nm thickness [Fig. 1(a)]. The typical Py material parameters (saturation magnetization $M_s = 860$ emu/cm³, exchange stiffness $A_{ex} = 1.3 \times 10^{-6}$ erg/cm, with zero magnetocrystalline anisotropy) were employed. The size of the individual cells was $2 \times 2 \times 30$ nm³, and the Gilbert damping constant was $\alpha = 0.01$. Static magnetic fields were applied perpendicularly to the dot plane, and the strength varied from $H_p = -3$ to 3 kOe at intervals of 1 kOe.¹⁹ The negative (positive) sign corresponds to the antiparallel (parallel) orientation of the core magnetization to the field direction.

III. RESULTS AND DISCUSSION

To examine how ω_0 varies with H_p , we used the following typical approach: first, we shifted the core from the center position by application of a static field of $H_y = 100$ Oe in the $+y$ direction; then, during free relaxation after the in-plane field was turned off, the averaged oscillations of the $m_x = M_x/M_s$ component ($\langle m_x \rangle$) were calculated as a function

^{a)}Author to whom correspondence should be addressed. Electronic mail: sangkoog@snu.ac.kr.

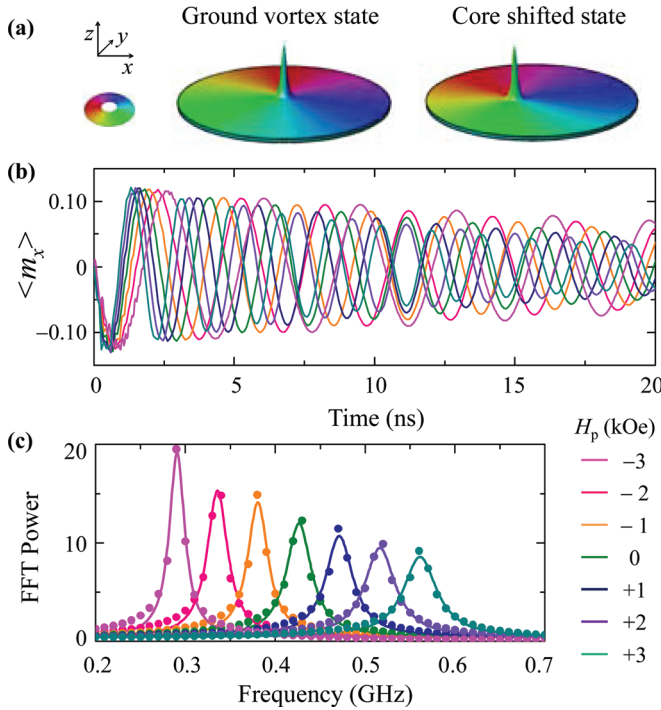


FIG. 1. (Color online) (a) Ground vortex state (left) and core-shifted state (right) with upward core magnetization and counter-clockwise (CCW) in-plane curling magnetization in Py disk of diameter $2R = 600$ nm and thickness $L = 30$ nm. The colors and heights represent the local in- and out-of-plane magnetization components, respectively. (b) Average m_x component $\langle m_x \rangle$ over whole disk vs time under perpendicular bias fields of indicated strength H_p , during relaxation process after vortex core is shifted. (c) FFT power spectra for different H_p values, obtained from FFTs of $\langle m_x \rangle$ oscillations over $t = 0$ -100 ns range.

of time for different H_p values [Fig. 1(b)]. Through fast Fourier transforms (FFTs) of the $\langle m_x \rangle$ oscillations, we plotted FFT powers in the frequency domain as a function of H_p , as shown in Fig. 1(c). The individual dominant frequency peaks represent $\omega_0/2\pi$ for a given H_p . The value of $\omega_0/2\pi$ at $H_p = 0$ is about 430 MHz, which increases monotonically to 560 MHz at $H_p = +3$ kOe and which decreases to 290 MHz at $H_p = -3$ kOe. The ω_0 variation with H_p (closed circles), as can be seen in Fig. 2, shows a linear dependence.

To understand such a linear response, we start with Thiele's analytical approach.¹⁶ Assuming a steady-state motion with core velocity \mathbf{v} , the governing equation of the gyrotropic mode is given as $-\mathbf{G} \times \mathbf{v} - \hat{D}\mathbf{v} + \partial W(\mathbf{X})/\partial \mathbf{X} = 0$, where $\mathbf{G} = -pG\hat{z}$ is the gyrovector with its constant $G > 0$ and the core polarization p , and $\hat{D} = D\hat{I}$ is the damping tensor with the identity matrix \hat{I} and its constant $D < 0$. The potential energy function is given as $W(\mathbf{X}) = W(0) + 1/2\kappa|\mathbf{X}|^2$ with the vortex-core position vector \mathbf{X} for a linear regime.¹¹ The first term is the potential energy for $\mathbf{X} = 0$, and the second, the potential energy of the intrinsic stiffness coefficient κ for displaced core position \mathbf{X} , as dominated by exchange and magnetostatic energies. Solving this governing equation, the characteristic angular eigenfrequency is given as $\omega_D = \kappa G/(G^2 + D^2)$ with a certain damping D .²⁰ For cases of negligible damping, that is, $G \gg |D|$, ω_D becomes approximately $\omega_0 = \kappa/G$.¹¹ Based on a two-vortex side surface charge free model,^{11,13,21} G and κ can be expressed explicitly as $G = 2\pi LM_s/\gamma$ with the gyro-

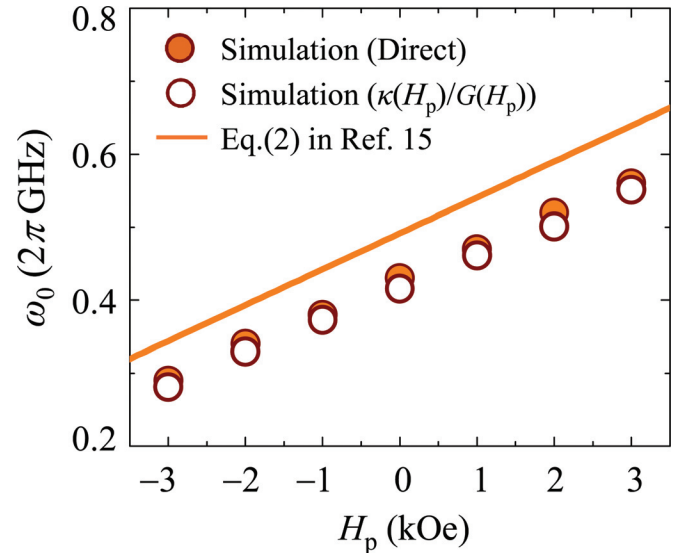


FIG. 2. (Color online) H_p dependence of ω_0 (closed circles), obtained from FFT power spectra [Fig. 1(c)], compared with results for $\kappa(H_p)/G(H_p)$ (open circles) obtained from H_p -dependent G and κ values (see Fig. 3), also obtained directly from simulation data. The solid line indicates the result of Eq. (2) reported in Ref. 15.

magnetic ratio γ , and $\kappa = \frac{40}{9}\pi M_s^2 L^2/R$ when $L/R \ll 1$. Accordingly, ω_0 is explicitly given as $\omega_0 = \frac{20}{9}M_s\gamma L/R$ (Ref. 13) and hence is determined only by the L/R aspect ratio for a given material. As such, the H_p dependence of ω_0 shown in Fig. 2 (closed circles) cannot be understood. Recently Loubens *et al.*¹⁵ reported an experimental result of the linear response, describing the result as an explicit expression of $\omega_0(H_p) = \omega_0(0)[1 + p(H_p/H_s)]$, where H_s is the field to saturate the dot along the normal (see solid line in Fig. 2). Our simulation results and the analytical expression were found to be in general agreement but with $\sim 14\%$ difference. The analytical form was estimated from the relation of $\omega_0 = \kappa/G$ (Ref. 11) for the case $H_p = 0$ by employing the estimated analytical forms $G(H_p) = G(0)[1 - p(H_p/H_s)]$ and $\kappa(H_p) = \kappa(0)[1 - (H_p/H_s)^2]$.¹⁵ However, such explicit expressions cannot properly be derived analytically due to the fact that because the application of H_p modifies the ground magnetization state of a vortex, the two-vortex side surface charge free model, which was used to derive analytical equations of G and κ at $H_p = 0$, cannot be applicable to the cases of application of perpendicular fields.

For a deeper or more correct understanding, the variations of G and κ with H_p should be calculated from the results of simulations in which variations of the vortex ground state with H_p are accounted for. Our main idea is to use the equivalent force balance equation $\mathbf{F}^G + \mathbf{F}^D + \mathbf{F}^W = 0$, where each term corresponds to the gyrotropic force, the damping force, and the restoring force due to the potential energy W , respectively, as indicated by the symbols in the superscript. The values of G and D can be extracted directly from those force terms $\mathbf{F}^G = pG\hat{z} \times \mathbf{v}$ and $\mathbf{F}^D = \hat{D} \cdot \mathbf{v} = D\mathbf{v}$, without any assumption, when the values of \mathbf{v} , \mathbf{F}^G , and \mathbf{F}^D are known. The force terms can be calculated from the simulation numerical data by $\mathbf{F}^G = \sum \mathbf{f}_i^G$ and $\mathbf{F}^D = \sum \mathbf{f}_i^D$ with $\mathbf{f}_i^G = (f_{i,x}^G, f_{i,y}^G)$, $\mathbf{f}_i^D = (f_{i,x}^D, f_{i,y}^D)$, where each term for the i th cell is given as

$$\begin{aligned} f_{i,x}^G &= -(1/\gamma M_s^2)(\mathbf{M} \times d\mathbf{M}/dt) \cdot \partial\mathbf{M}/\partial x, \\ f_{i,y}^G &= -(1/\gamma M_s^2)(\mathbf{M} \times d\mathbf{M}/dt) \cdot \partial\mathbf{M}/\partial y, \end{aligned} \quad (1a)$$

$$\begin{aligned} f_{i,x}^D &= -(\alpha/\gamma M_s)(d\mathbf{M}/dt) \cdot \partial\mathbf{M}/\partial x, \\ f_{i,y}^D &= -(\alpha/\gamma M_s)(d\mathbf{M}/dt) \cdot \partial\mathbf{M}/\partial y. \end{aligned} \quad (1b)$$

The calculation results (open circles) for G as functions of H_p , using the approach explained in the preceding text, are shown in Fig. 3(a). The slope of $\Delta G/\Delta H_p$, plotted in Fig. 3(a), is about -9.8×10^{-11} erg·s/(cm²·kOe). The negative sign indicates that G decreases with increasing H_p . This is consistent with the fact that G is determined by the relative magnitude of the out-of-plane magnetization of the core with respect to those around it.¹⁶ This variation is in good agreement (within a 6% difference) with the explicit expression (solid line) $G(H_p) = G(0)[1 - p(H_p/H_s)]$ with $G(0) = 2\pi L M_s/\gamma$ (Ref. 11) for $\gamma = 2\pi \times 2.8$ MHz/Oe, $L = 30$ nm, and $H_s = 10$ kOe, as obtained for our nanodot dimensions.

The calculation results of D are shown in Fig. 3(b). D increases with increasing H_p but deviates slightly from the linear response in the negative H_p region. $D = -2.1402 \times 10^{-11}$ erg·s/cm² at $H_p = 0$ is close to the value -2.3016×10^{-11} erg·s/cm² obtained from the analytic equation $D = -\alpha\pi M_s L [2 + \ln(R/R_c)]/\gamma$ (Ref. 22) for $R = 300$ nm and $L = 30$ nm and assuming the vortex-core radius $R_c = 15$ nm. This equation was derived for the case of $H_p = 0$ based on the model proposed by Usov *et al.*²³ The $G \gg |D|$ results plotted in Fig. 3 indicate that the damping term only negligibly contributes to the eigenfrequency.

Next, the H_p dependence of the κ value was numerically calculated from the simulation data using $W(\mathbf{X}) = W(0) + 1/2\kappa|\mathbf{X}|^2$. To calculate the total potential energy W versus

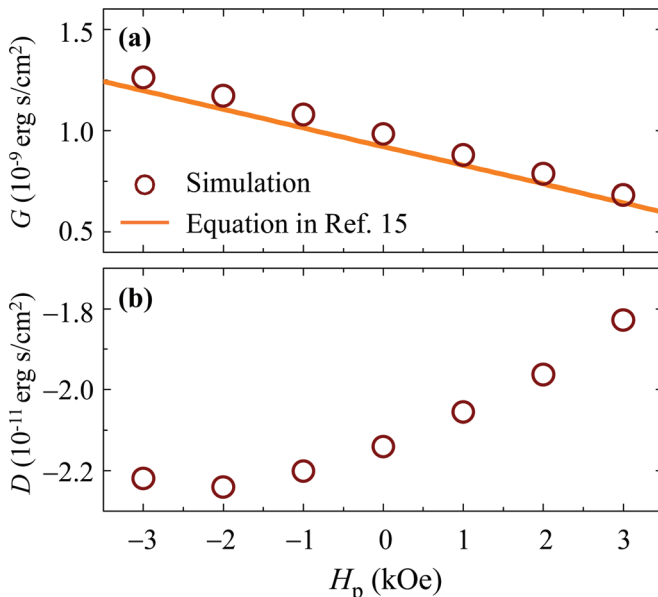


FIG. 3. (Color online) Dependences of dynamic variables G and D on H_p . The open circles show the simulation results obtained through $G = p|\mathbf{F}^G|/|\mathbf{v}|$, $D = |\mathbf{F}^D|/|\mathbf{v}|$. The solid line corresponds to the result obtained from an explicit expression of $G(H_p) = G(0)[1 - p(H_p/H_s)]$, as reported in Ref. 15, where $H_s = 10$ kOe was used for our nanodot dimensions.

$X = |\mathbf{X}|$, the vortex core was shifted from the initial center position and then relaxed, as shown in Fig. 1(b). The slope in the plot of W versus X^2 accordingly gives rise to $\kappa/2$, as seen in Fig. 4(a). The resultant H_p -dependent κ values are shown in Fig. 4(b) (see open circles). The value of κ at $H_p = 0$ is estimated to ~ 2.635 erg/cm², which value is smaller by 11% than that of the analytical expression reported in Refs. 11 and 13. This seems that the analytical expression has been derived assuming the two-vortices model^{11,13,21} that is different from dynamic vortex configurations in the simulations. The κ value decreases with increasing $|H_p|$, and the parabolic curve is somewhat asymmetric at about $H_p = 0$ in contrast to the explicit parabolic expression (solid line) of $\kappa(H_p) = \kappa(0)[1 - (H_p/H_s)^2]$ reported in Ref. 15. This explicit form was obtained for the assumption that the potential energy profiles are the same for the different signs of $+H_p$ and $-H_p$. The asymmetry of our result originates from the difference in the m_z profile of the vortex core between $+H_p$ and $-H_p$, shown in the inset of Fig. 4(b). This appears to break the symmetry of κ at around $H_p = 0$. The difference in ω_0 between our simulation results (closed circles) and the analytical estimation (solid line) in Ref. 15 can be ascribed mainly to the difference in κ : $\kappa(-3$ kOe) = 2.232 erg/cm², $\kappa(+3$ kOe) = 2.365 erg/cm², from our simulation, and $\kappa(-3$ kOe) = $\kappa(+3$ kOe) = 2.591 erg/cm², from the analytical equation. The core m_z profiles not considered in the analytical expression would give rise to incorrect values of κ for positive and negative H_p values as can be evidenced by excellent agreements between the simulation results of $\omega_0(H_p)$ (closed circles) and the results of $\kappa(H_p)/G(H_p)$ (open circles), shown in Fig. 2.

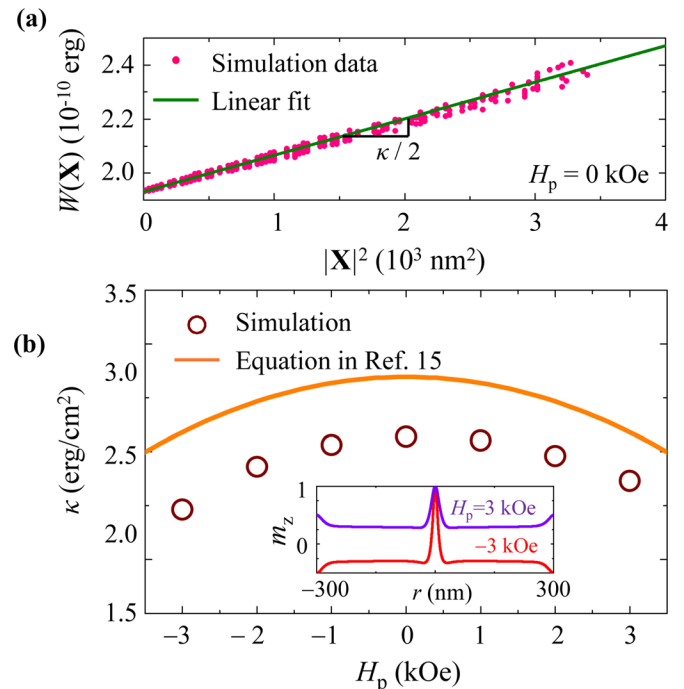


FIG. 4. (Color online) (a) Calculated total energy $W(\mathbf{X})$ vs $|\mathbf{X}|^2$ for $H_p = 0$ kOe. The solid line indicates a linear fit to the simulation results (dots). (b) Dependence of κ on H_p . The open circles indicate values obtained directly from the simulation results, while the solid line corresponds to the result for $\kappa(H_p) = \kappa(0)[1 - (H_p/H_s)^2]$ reported in Ref. 15. The inset shows the comparison of the core-region m_z profiles for $H_p = +3$ and -3 kOe.

IV. CONCLUSIONS

We studied, by micromagnetic simulations combined with an analytical approach, the dependence of the angular frequency of vortex core oscillations upon H_p . The observed linear increase of the vortex eigenfrequency with H_p could be explained quantitatively in terms of the H_p dependences of all of the vortex dynamic variables, G , κ , and D , calculated numerically from the micromagnetic simulation results. This work shows how numerical simulations and their quantitative interpretations promise a more correct understanding of vortex dynamics in nanodots.

ACKNOWLEDGMENTS

This work was supported by the Basic Science Research Program through the National Research Foundation of Korea (NRF) funded by the Ministry of Education, Science and Technology (No. 20100000706).

- ¹A. Hubert and R. Schäfer, *Magnetic Domains* (Springer-Verlag, Berlin, 1998).
- ²T. Shinjo, T. Okuno, R. Hassdorf, K. Shigeto, and T. Ono, *Science* **289**, 930 (2000).
- ³B. Van Waeyenberge, A. Puzic, H. Stoll, K. W. Chou, T. Tyliczszak, R. Hertel, M. Fähnle, H. Brückl, K. Rott, G. Reiss, I. Neudecker, D. Weiss, C. H. Back, and G. Schütz, *Nature* **444**, 461 (2006).
- ⁴K. Yamada, S. Kasai, Y. Nakatani, K. Kobayashi, H. Kohno, A. Thiaville, and T. Ono, *Nat. Mater.* **6**, 269 (2007); S.-K. Kim, Y.-S. Choi, K.-S. Lee, K. Y. Guslienko, and D.-E. Jeong, *Appl. Phys. Lett.* **91**, 082506 (2007).
- ⁵S. Choi, K.-S. Lee, K. Yu. Guslienko, and S.-K. Kim, *Phys. Rev. Lett.* **98**, 087205 (2007).
- ⁶Q. F. Xiao, J. Rudge, E. Girgis, J. Kolthammer, B. C. Choi, Y. K. Hong, and G. W. Donohoe, *J. Appl. Phys.* **102**, 103904 (2007); R. Hertel, S. Gliga, M. Fähnle, and C. M. Schneider, *Phys. Rev. Lett.* **98**, 117201 (2007).
- ⁷K.-S. Lee, K. Yu. Guslienko, J.-Y. Lee, and S.-K. Kim, *Phys. Rev. B* **76**, 174410 (2007); K. Y. Guslienko, K.-S. Lee, and S.-K. Kim, *Phys. Rev. Lett.* **100**, 027203 (2008).
- ⁸R. P. Cowburn, *Nat. Mater.* **6**, 255 (2007); J. Thomas, *Nature Nanotech.* **2**, 206 (2007).
- ⁹Y.-S. Choi, M.-W. Yoo, K. -S. Lee, Y.-S. Yu, H. Jung, and S.-K. Kim, *Appl. Phys. Lett.* **96**, 072507 (2010).
- ¹⁰S.-K. Kim, K.-S. Lee, Y.-S. Yu, and Y.-S. Choi, *Appl. Phys. Lett.* **92**, 022509 (2008).
- ¹¹K. Yu. Guslienko, B. A. Ivanov, V. Novosad, H. Shima, Y. Otani, and K. Fukamichi, *J. Appl. Phys.* **91**, 8037 (2002).
- ¹²A. Dussaux, B. Georges, J. Grollier, V. Cros, A. V. Khvalkovskiy, A. Fukushima, M. Konoto, H. Kubota, K. Yakushiji, S. Yuasa, K. A. Zvezdin, K. Ando, and A. Fert, *Nat. Commun.* **1**, 8 (2010).
- ¹³K. Yu Guslienko, X. F. Han, D. J. Keavney, R. Divan, and S. D. Bader, *Phys. Rev. Lett.* **96**, 067205 (2006).
- ¹⁴Y.-S. Choi, S.-K. Kim, K.-S. Lee, and Y.-S. Yu, *Appl. Phys. Lett.* **93**, 182508 (2008); Y.-S. Choi, K.-S. Lee, and S.-K. Kim, *Phys. Rev. B* **79**, 184424 (2009).
- ¹⁵G. de Loubens, A. Riegler, B. Pigeau, F. Lochner, F. Boust, K. Y. Guslienko, H. Hurdequint, L. W. Molekamp, G. Schmidt, A. N. Slavin, V. S. Tiberkevich, N. Vukadinovic, and O. Klein, *Phys. Rev. Lett.* **102**, 177602 (2009).
- ¹⁶A. A. Thiele, *Phys. Rev. Lett.* **30**, 230 (1973); D. L. Huber, *Phys. Rev. B* **26**, 3758 (1982).
- ¹⁷We used the 1.2a4 version of the OOMMF code. See <http://math.nist.gov/oommf>.
- ¹⁸L. D. Landau and E. M. Lifshitz, *Phys. Z. Sowjetunion* **8**, 153 (1935); T. L. Gilbert, *Phys. Rev.* **100**, 1243 (1955).
- ¹⁹At fields smaller than $H_p = -3$ kOe, it is too difficult to investigate vortex-core reversals as they are very unstable.
- ²⁰K.-S. Lee and S.-K. Kim, *Phys. Rev. B* **78**, 014405 (2008).
- ²¹K. L. Metlov and K. Y. Guslienko, *J. Magn. Magn. Mater.* **242**, 1015 (2002).
- ²²K. Yu. Guslienko, *Appl. Phys. Lett.* **89**, 022510 (2006).
- ²³N. A. Usov, and S. E. Peschany *J. Magn. Magn. Mater.* **118**, L290 (1993).